INFLUENCE OF CARBIDE-PROMOTING ELEMENTS ON THE PEARLITE CONTENT AND THE TENSILE PROPERTIES OF HIGH SILICON SSDI DUCTILE IRON

Moritz Riebisch [ID], Hergen Groß Sönke, Björn Pustal, and Andreas Bührig-Polaczek
Foundry Institute, Rheinisch-Westfälische Technische Hochschule Aachen, Aachen, Germany

Abstract

Steel scrap is one of the most important raw materials for the production of ductile iron (DI) because of its low cost. Most low alloyed steels contain carbide-promoting elements such as chromium, manganese, molybdenum and niobium and are currently not used for the production of DI because of their negative impact on the mechanical properties. The solid solution strengthened DI grades (SSDI) exhibit an increased tolerance toward carbide-promoting elements and thus allow the production of ferritic DI using low alloyed steel scrap. Therefore, the tolerance limits of these elements need to be identified. The following article shows the influence of low contents of Cr, Mn, Mo and Nb on the microstructure and the tensile properties of the SSDI grade EN-GJS-500-14. The results indicate that even low levels of chromium and molybdenum have a negative impact on tensile properties, whereas manganese and niobium are tolerable up to much higher levels.

Keywords: solid solution strengthened ductile iron SSDI, carbide-promoting elements, microstructure, pearlite, tensile properties

Introduction

Ductile iron (DI) has been industrially produced for approximately 60 years. The benefits of this material are the excellent castability, ductility, cost–performance ratio and its versatility. It is used for wind turbine components, safety components in cars, storing and transportation devices for nuclear waste and many other applications. Apart from pig iron, steel scrap is the most important raw material for DI production because of its low cost. Low alloyed steel scrap is usually avoided since it contains carbide-promoting elements which have a negative impact on the microstructure and the mechanical properties. Especially in castings with a high solidification time, the presence and segregation of these elements lead to the formation of pearlite and carbides in the microstructure. Since the steel industry constantly develops new high-strength steel grades with an increased level of carbide-promoting elements, the long-term quality of available steel scrap will change. Therefore, new possible applications for low alloyed steel scrap in ductile iron production must be developed to perpetuate the cost advantage and the excellent mechanical properties of DI.

The new solution strengthened ductile iron grades with a silicon content up to 4.3 wt% exhibit a unique combination of strength and ductility.[1] The high silicon levels promote a full ferritic matrix and therefore good mechanical properties and machinability. Another advantage of the high silicon level is the increased tolerance against carbide-promoting elements, as it was shown by Löblich et al.[2] To repeatedly achieve a SSDI grade with the desired mechanical properties under the use of low alloyed steel scrap, the limit of tolerance for the different carbide-promoting elements must be identified. Therefore, investigations with different levels of Cr, Mn, Mo and Nb in the ductile iron grade GJS-500-14 with a nominal Si content of 3.8 wt% were carried out. The microstructure and the tensile properties were investigated in order to find tolerable levels of these elements in this SSDI grade.

State of the Art

The individual and combined effect of different carbide-promoting elements on the microstructure and the mechanical properties of DI has been investigated for

several decades. Rivera et al.[3] analyzed the impact of niobium contents up to 0.366 wt% on the properties of ductile iron. Niobium slightly increases the amount of pearlite in the matrix and thus leads to a moderate increase in strength and a decrease in elongation. Hernandez-Avila et al.[4] found a similar effect for molybdenum contents up to 0.38 wt% regarding the mechanical properties of DI. Furthermore, molybdenum induces a refinement of the pearlite structure. An overview of the impact of different pearlite and carbide-promoting elements in ductile iron is given by Hasse.[5] An extensive design of experiment is necessary to investigate the combined effect of several elements. Campomanes and Goller used a factorial design of experiment to analyze the individual and combined impact of the elements Si, Mn, Cr, Ti and V on the microstructure of DI.[6] The results revealed a strong impact of Cr and Mn on the amount of pearlite and carbides, whereas a higher amount of Si counteracts the effect of the other elements. An identical design of experiment was used by Wolf et al.[7] to study the influence of Mn, Cr, Nb, V and B on the microstructure and mechanical properties of ferritic ductile iron EN-GJS-400-15 in cast parts with various wall thickness. Their results showed that a higher solidification time in thick-walled castings leads to more carbides induced by segregation and thus to an increased degradation of mechanical properties. Such a factorial design of experiment is of limited suitability for the determination of tolerance limits since the percentage of each element is usually changed only from a low to a rather high value. Furthermore, the limits of tolerance depend on the solidification time and thus on the wall thickness of the casting. Möx and Menk[8] specify the tolerance limits for Mn, Nb and V in conventional DI castings with wall thicknesses between 5 and 30 mm. According to their investigations, the limits for these elements are 0.3, 0.05 and 0.1 wt%, respectively. It was partly shown by Löblich et al.[2] that the

tolerance limits for these and other carbide-promoting elements in solution strengthened ductile iron are considerably higher. In the present study, further investigations with different levels of Mn, Cr, Mo and Nb in castings with different solidification times have been executed to define tolerable percentages of these elements for the production of SSDI.

Experimental Design

In this study, near-eutectic SSDI was alloyed with different percentages of Mn, Cr, Mo and Nb and the effect on the microstructure and the tensile properties was analyzed for different solidification times. Both the individual and the combined effects of Mn with the other three elements were investigated because Mn is the most commonly used alloying element in steel, and thus, its interdependency with other elements is relevant. Casting no. 1 is the base SSDI without additional alloying elements. Castings nos. 5, 7 and 12 are combined factor trials with an addition of 0.5% Mn and a second element. The remaining castings are single factor trials with one alloying element. The chemical compositions of the melt for all experiments are listed in Table 1. The carbon content C_{TA} was determined via cooling curve thermal analysis. The percentage of the other elements was measured with a spark emission spectrometer.

To study the influence of the solidification time on the amount of pearlite and carbides, a casting geometry was used including three cast parts with different solidification times. The geometry included two Y wedges, one of type II (wall thickness 25 mm) and one of type IV (wall thickness 75 mm), and a cylindrical cast part with a diameter of 140 mm. An insulating riser sleeve was used for the

Table 1. Chemical Composition of the Experimental Test Castings in wt%.

Cast no.	C_{TA} (%)	Si (%)	Cr (%)	Mn (%)	Mo (%)	Nb (%)	Mg (%)
1	3.02	4.02	0.043	0.172	0.003	0.003	0.028
2	2.95	3.82	0.044	*0.519*	0.003	0.004	0.045
3	2.85	4.21	0.044	0.178	*0.268*	0.004	0.036
4	2.87	3.96	0.045	0.176	*0.535*	0.003	0.028
5	2.88	4.00	0.046	*0.536*	*0.528*	0.003	0.023
6	2.89	3.88	0.041	0.189	0.004	*0.180*	0.040
7	2.98	3.98	0.044	*0.530*	0.003	*0.237*	0.034
8	2.84	4.12	0.045	0.180	0.004	*0.392*	0.035
9	2.88	4.26	*0.094*	0.178	0.002	0.003	0.036
10	2.97	4.12	*0.294*	0.177	0.004	0.003	0.032
11	3.05	4.06	*0.624*	0.180	0.004	0.003	0.032
12	2.91	4.11	*0.612*	*0.532*	0.004	0.003	0.043

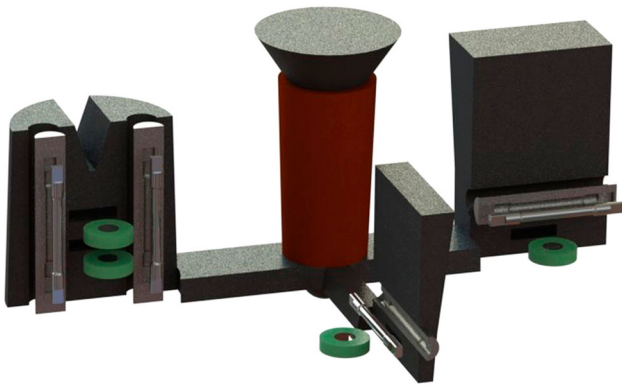The alloyed carbide-promoting elements are italicized

Figure 1. Geometrical arrangement of the three cast parts inside of the sand mold. Tensile test bars and samples for metallography are taken from each casting.
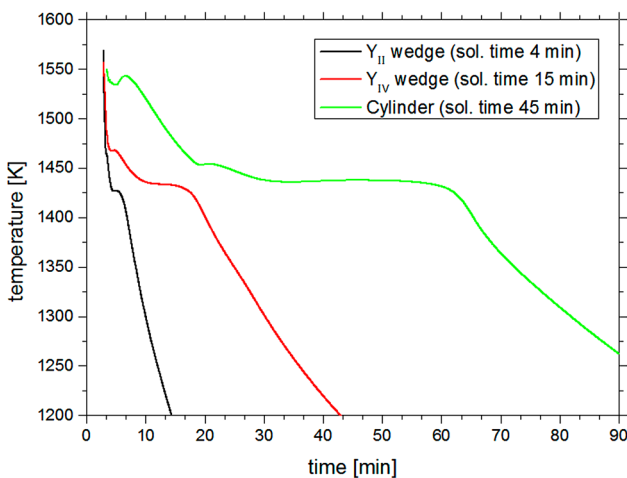

Figure 2. Cooling curves recorded in the center of the test castings to calculate the solidification time.

cylinder to increase the solidification time. The arrangement of the cast parts in the sand mold is shown in Figure 1. The locations of the samples for metallographic preparation and for the tensile test bars are also depicted. The sand mold was of cylindrical shape with a diameter of 600 mm. The gating system is located in the center.

The solidification time of each cast part was measured in its thermal center with type K thermocouples during solidification of melt no. 1. The cooling curves are presented in Figure 2. The solidification time is the interval between the moment where *T* falls below the liquidus temperature and the end of solidification. Solidification times for Y_{II} wedge, Y_{IV} wedge and cylinder are 4, 15 and 45 min, respectively.

Experimental Procedure

The sand molds were produced with furan-resin-bonded silica sand. The raw materials for the manufacturing of the melt consisted of recycled iron EN-GJS-400-15 from Georg Fischer GmbH and commercial high-purity iron.

This results in a base melt with a very low level of carbide-forming elements. The silicon percentage and the percentage of the carbide formers were adjusted with different ferroalloys. The materials were melted in a 50-kg graphite crucible with a medium-frequency induction furnace. The melt was superheated to 1770 K (1500 °C) for 10 min, and slag was removed afterward. Then the magnesium treatment was performed with a cerium-free FeSiMg master alloy in a plunger at a temperature of approximately 1720 K (1450 °C). After the nodularization treatment and a second slag removal, the melt in the crucible was inoculated with 0.2 wt% of a ferrosilicon-based inoculant whose composition contains calcium, rare earth metals and bismuth. After the inoculation, a small amount of the melt was used for the cooling curve thermal analysis and for the production of a chilled sample for the chemical analysis in the spark emission spectrometer. Then, the melt was poured into the sand mold with a casting temperature of approximately 1620 K (1350 °C). The casting then cooled for 24 h before unpacking.

Sample Preparation and Analysis

After unpacking, the three cast parts were first cut from the runner with an angle grinder. The samples for metallographic analysis were cut out of the castings with a bow saw and a water-cooled disk cutter. After embedding, the metallographic specimens were ground with silicon carbide sandpaper with different grits (180, 320, 500 and 1000) and polished with diamond polish (size 9, 3 and 0.25 micron). Grinding and polishing took place in an automatic buffing machine. For the quantitative analysis of graphite morphology, five images were taken from every specimen in the polished state with a digital light microscope. The magnification factor for graphite analysis was 100, and a digital resolution of 2600 × 2060 pixels was used. The image processing software Axiovision KS 400 was used for the quantitative evaluation of graphite morphology. The shape factors roundness and compactness were used for the graphite particle classification according to the work of Velichko.[9] The shape factors were used to divide the graphite particles into class I through VI. The classification limits for each shape class depend on the size of the particle.[10] In the present work, the following formula was used for the calculation of nodularity *N*:

$$N = \frac{\sum_{VI} A_i + \frac{1}{2}\sum_{IV}^{V} A_i}{\sum_{I}^{VI} A_i} \qquad \text{Eqn. 1}$$

The area A_i of the round particles is added together, and the result is divided by the total area of graphite particles. The shape classes IV and V are weighted with a factor of ½ since their shape is irregular. For the determination of the pearlite content, the specimens were etched with alcoholic nitric acid. Five microscopic pictures were taken from each etched sample with the same parameters as for the graphite

analysis. Figure 3 shows an exemplary picture of a specimen after etching. The pearlite has a dark coloration after the etching procedure.

Due to its dark coloring, the pearlite cannot be graphically separated from the graphite without error. Instead, the joint area percentage of graphite %G and pearlite %P is determined from the etched sample pictures. The graphite area percentage that was identified from the polished sample pictures is then subtracted from the joint area percentage to calculate the amount of pearlite in each sample.

$$\%P = (\%G + \%P)_{\text{etched}} - \%G_{\text{polished}} \qquad \text{Eqn. 2}$$

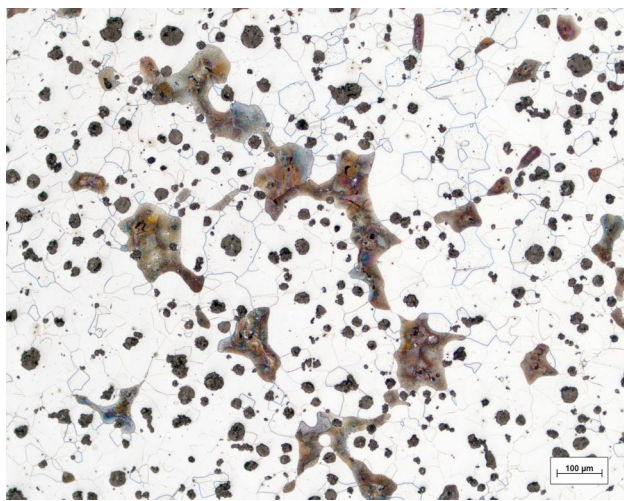The tensile properties in each cast part were tested for every casting with a pearlite content up to 20% to check whether mechanical properties that fulfill the requirements in the standard DIN EN 1563, where a maximum perlite content of 5% is defined for SSDI, can be achieved with higher pearlite percentages. The removal of the tensile test bars was performed with a water-cooled hollow drill. The test bars of shape A with a diameter of 8 mm, according to DIN EN 50125, were then manufactured from the drilling cores with a lathe. One test bar for each Y_{II} and Y_{IV} wedge and two test bars for each cylinder were tested.

Results and Discussion

Microstructure

All microstructural characterization results are summarized in Table 2. The strong impact of the solidification time on nodule count and nodularity is visible in the results of the quantitative graphite analysis. In agreement with the results of Górny and Tyrala,[11] the nodule count increased with increasing cooling rate. The nodule count in the Y wedge type II is usually between 400 and 500 nodules/mm². The Y wedge type IV shows an average nodule count of approximately 300 nodules/mm², and in the cylindrical casting the nodule count is roughly 100/mm². No interaction between the residual Mg content in the melt and the nodule count was found, whereas the nodularity shows a direct proportionality to the Mg content in all cast parts because the amount of irregular graphite declines. The nodularity in the Y_{II} wedge lies between 80 and 90% in the majority of cases, and in the Y_{VI} wedge it is usually between 75 and 85%. The nodularity in the cylinder exhibits great fluctuations which is due to the increased grain size that involves a higher tendency to degraded graphite shapes. Usually, the nodularity is in the range from 60 to 75%.

Figure 3. Microstructure in the Y wedge type IV of Cast no. 10 after etching with nitric acid.

Table 2. Results of Microstructure Characterization for all Analyzed Cast Parts.

Cast no.	Y wedge type II			Y wedge type IV			Cylinder		
	Nod. count (1/mm²)	Nodularity (%)	Pearlite (%)	Nod. count (1/mm²)	Nodularity (%)	Pearlite (%)	Nod. count (1/mm²)	Nodularity (%)	Pearlite (%)
1	415	76	2.0	242	72	2.4	136	72	4.4
2	421	88	6.0	268	86	4.5	105	74	6.1
3	443	90	0.3	261	81	4.6	95	68	3.2
4	422	89	11.0	226	76	11.8	89	62	9.4
5	302	73	14.8	216	67	15.8	76	57	15.6
6	414	87	0.0	240	83	0.0	106	79	4.0
7	343	85	8.3	231	77	8.3	87	60	11.1
8	351	72	5.9	225	62	5.7	110	71	7.1
9	564	87	0.8	361	82	2.6	159	71	3.9
10	487	81	10.7	291	77	13.6	117	73	14.0
11	301	80	37.9	293	80	40.0	89	59	41.8
12	404	86	49.2	247	70	49.1	90	62	50.7

Cast no.	Y wedge type II			Y wedge type IV			Cylinder		
	$R_{p0.2}$ (MPa)	R_m (MPa)	A (%)	$R_{p0.2}$ (MPa)	R_m (MPa)	A (%)	$R_{p0.2}$ (MPa)	R_m (MPa)	A (%)
1	422	548	16.85	417	539	18.45	412	524	12.19
2	434	562	16.89	427	555	17.19	419	529	9.16
3	444	574	16.2	436	563	13.61	426	532	6.93
4	432	577	15.49	427	578	13.41	412	523	5.68
5	450	600	12.57	437	585	12.01	429	505	1.94
6	446	570	17.77	439	565	17.01	428	544	12.52
7	432	577	18.39	425	565	12.04	416	538	10.85
8	440	576	17.23	432	558	16.24	419	534	8.81
9	439	565	18.31	432	554	15.15	424	534	10.64
10	447	597	16.03	438	581	12.45	431	546	5.53

The pearlite content in all samples analyzed was between 0 and 50%. Chromium shows the strongest impact on the ferrite/pearlite ratio. At a Cr content of 0.6%, the pearlite level reaches 37.9% in the Y_{II} wedge and 41.8% in the cylinder. With a lower Cr level of 0.3%, a pearlite level between 10.4 and 14.0% was reached. A slight increase in the pearlite level with increasing solidification time was found in both cases. The other alloyed elements, manganese, molybdenum and niobium, did not show such a clear relation between these two quantities. Furthermore, the tendency to produce pearlite is much weaker for the other elements. The addition of 0.5 wt% Mn into the melt leads to a pearlite content between 4.5 and 6.1% so that the tolerance level of 5% pearlite in the matrix according to DIN EN 1563 is just slightly exceeded. When Mn is added together with another element, the additional growth of pearlite is stronger compared to the exclusive addition of 0.5 wt% Mn. An identical addition of molybdenum generates a pearlite content between 9.4 and 11.8%. When the Mo level is lowered to 0.25 wt%, the pearlite level does not exceed 5% in any of the three cast parts. This threshold value is also held for a niobium addition of 0.2 wt%. A doubling of the Nb addition or an additional increase in the Mn level leads to a pearlite level higher than 5% (c.f. Cast nos. 7 and 8). The amount of carbides in the microstructure, which is not listed in Table 2, has a maximum of 0.42% in the castings analyzed and is thus much lower than the threshold value of 1% cementite as given in the standard EN ISO 1563. A significant impact of the carbide level on the static mechanical properties could not be determined, and therefore, the carbide content is neglected in the following discussion.

Tensile Properties

The static mechanical properties of SSDI are defined by the solid solution strengthening effect, the composition of the metallic matrix and the graphite morphology. An increasing pearlite content in the matrix results in an increasing tensile strength and a reduced ductility.[12,13] An improved nodularity leads to an increased tensile strength and a higher elongation at fracture.[14] An increased nodule count also leads to a general improvement of the mechanical properties.[15,16] The influence of the alloying elements on the mechanical properties is fundamentally given by their tendency to form pearlite and carbides.[7] The tensile properties of all tested castings are listed in Table 3.

The influence of pearlite content on the tensile properties is shown in Figure 4. Although the nodularity varies in the three used casting parts within the performed experiments, the main impact on the mechanical properties is given by the pearlite content. The tensile strength R_m increases with a growing amount of pearlite as expected. The gain of strength is smaller for longer solidification times. In the cylindrical casting, there is almost no increase in tensile strength. The yield strength $R_{p0.2}$ does not show a consistent correlation with the pearlite content. The ratio $R_{p0.2}/R_m$ decreases with an increasing pearlite percentage. For the highest pearlite percentages analyzed, the cylindrical sample shows a huge deviation from this linearity. This arises from the change of fracture behavior from ductile to brittle as found in the cylinder at corresponding amounts of pearlite. This leads to a lower maximum tensile strength and an enormous drop of elongation at fracture below 2%. The elongation at fracture A in the cylinder responds more sensitively to the pearlite in the matrix than in the other cast parts where A is still above a value of 12% at the highest pearlite content. The cause for this observation is the intensified segregation of the pearlite-forming elements arising from the bigger grain size and the slower cooling of the casting. This leads to an inhomogeneous distribution of pearlite and thus to reduced tensile properties.
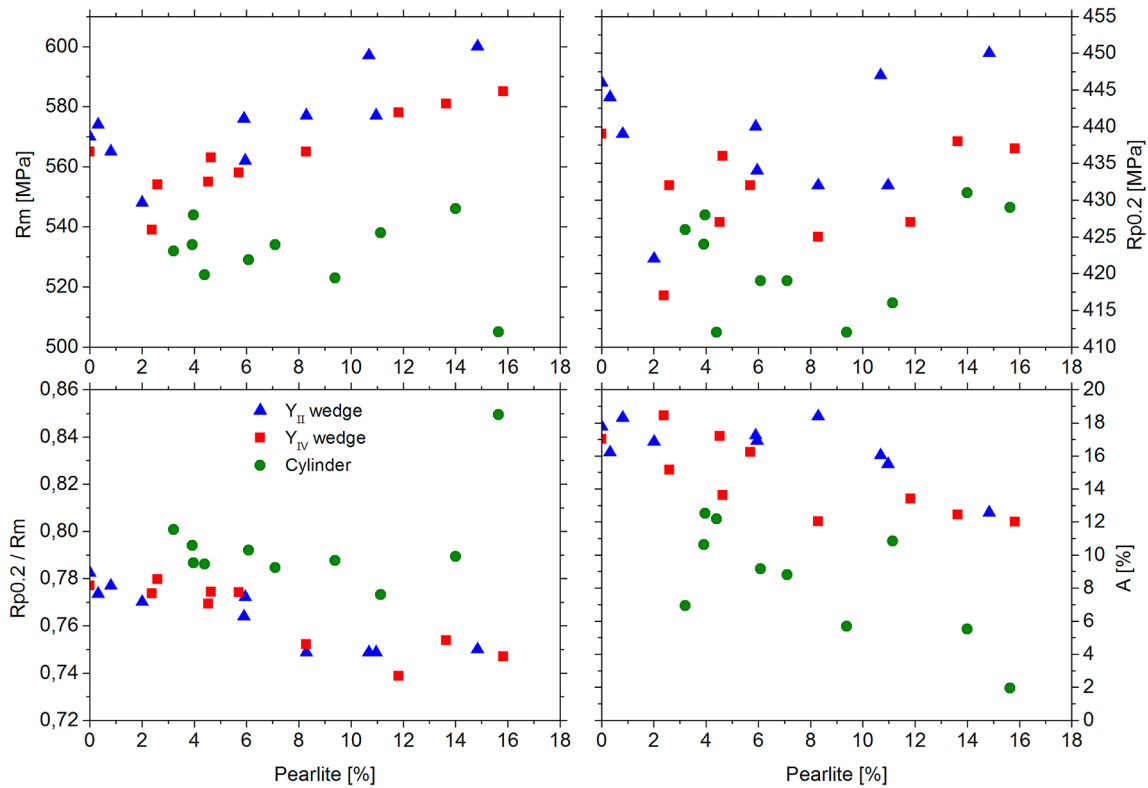
Figure 4. Correlation between pearlite content and tensile properties for the test castings.

Conclusions

The aim of this work was to analyze the influence of certain pearlite and carbide-promoting elements on the microstructure and the tensile properties of SSDI cast parts with different solidification times to identify tolerance limits for the production process. The results allow the following conclusions to be made:

1. The elements manganese and niobium are weak pearlite promoters, and their addition leads to an increased tensile strength and yield strength. No decline of elongation was detected for an addition of 0.2% niobium in all three casting parts. For an addition of 0.5% manganese, the elongation at fracture dropped slightly in the Y_{IV} wedge and the cylinder. No degradation occurred in the Y_{II} wedge; thus, a Mn level of 0.5% is tolerable for solidification times below 15 min.

2. A molybdenum addition up to 0.25% does not lead to a critical increase in pearlite in the microstructure for solidification times between 4 and 45 min. Nevertheless, the elongation at fracture clearly decreases for solidification times above 15 min. For a solidification time of 4 min, an amount of 0.25% Mo is tolerable. A strengthening in conjunction with the Mo-addition occurs as can be seen by comparison of Cast nos. 1 and 4.

3. Chromium is a strong pearlite promoter. A Cr level of 0.3% leads to a pearlite level above 10%

in all three casting parts. This decreases the elongation considerably for a solidification time of 15 min or larger. This result disagrees with former publications, where a chromium content of 0.3% has been classified as unproblematic for SSDI with similar Si contents.[2] According to the present work, a chromium level of 0.1% or less does not increase the pearlite content of SSDI and is tolerable according to the tensile test data for a wall thickness of 25 mm.

The results indicate that some elements like manganese or niobium can be tolerated in SSDI in considerable amounts, but they depend on the solidification time. This allows the use of certain alloyed steel scraps for a cost-efficient production of this innovative and multifunctional material. Other elements, chromium in the first instance, have an enormous negative impact on the microstructure and the mechanical properties. Their amount has to be kept on a low level, especially in castings with a solidification time of 45 min or larger. The influence of the solidification time on the tolerance limit of different carbide-promoting elements in SSDI was clearly demonstrated in the work presented.

Acknowledgements

REFERENCES

1. H. Löblich, Gusseisen mit Kugelgraphit profitiert vom hohen Siliziumgehalt. Masch. Markt **41**, 42–46 (2011)

2. H. Löblich, W. Stets, G. Gassner et al., Hoch siliciumhaltiges Gusseisen mit Kugelgraphit toleriert größere Anteile an carbidbildenden Elementen. Giesserei **99**(4), 28–32 (2012)

3. I. Rivera, A. Roca, F. Patiño et al., Microalloyed niobium influence on ductile ferrite cast iron. Int. J. Cast Met. Res. **16**(1–3), 65–70 (2003)

4. J. Hernandez-Avila, E. Salinas-Rodriguez, E. Cerecedo-Saenz et al., The effect of molybdenum on the microstructure of nodular iron. Eur. Sci. J. **11**(36), 337 (2015)

5. S. Hasse, Niedriglegiertes Gusseisen mit Kugelgraphit. Gießerei-Praxis **8**(Niedriglegiertes GJS), 293–301 (2005)

6. E. Campomanes, R. Goller, The effect of certain carbide promoting elements on the microstructure of ductile iron. AFS Trans. **87**, 619–626 (1979)

7. G. Wolf, W. Stets, U. Petzschmann, Bewertung der kumulativen Wirkung von Carbid bildenden Elementen auf die Eigenschaften von GJS-400-15. Gießerei **10**(Technologie & Trends), 24–32 (2011)

8. C. Möx, W. Menk, Risiken und Grenzen beim Einsatz mikrolegierten Stahlschrotts für Gußeisen mit Kugelgraphit. Giessereiforschung **11**(12), 301–307 (1994)

9. A. Velichko, F. Mücklich, Neue Möglichkeiten der objektiven Graphitklassifizierung in Gusseisen durch Nano-Tomographie und internetbasierte Online-Verfahren. VDI-Ber. **1949**, 21–36 (2007)

10. A. Velichko, *Quantitative 3D Characterization of Graphite Morphologies in Cast Iron using FIB Microstructure Tomography* (Pharmazie, Bio- und Werkstoffwissenschaften, Universität des Saarlandes, Saarbrücken, Naturwissenschaftlich-Technische Fakultät III Chemie, 2008)

11. M. Gorny, E. Tyrala, Effect of cooling rate on microstructure and mechanical properties of thin-walled ductile iron castings. J. Mater. Eng. Perform. **22**(1), 300–305 (2013)

12. R.A. Gonzaga, Influence of ferrite and pearlite content on mechanical properties of ductile cast irons. Mater. Sci. Eng., A **567**, 1–8 (2013)

13. M. Hafiz, Mechanical properties of SG-iron with different matrix structure. J. Mater Sci **36**, 1293–1300 (2001)

14. R.B. Gundlach, *Nodularity its Measurement and its Correlation with the Mechanical Properties of Ductile Iron* (Stork Climax Research Services, Wixom, 2006)

15. T. Hareyama, H. Horie, T. Kowata et al., Effects of graphite nodule count and pearlite lamellar spacing on mechanical properties of fine pearlite spheroidal graphite cast iron. J. Jpn. Foundry Eng. Soc. **76**(11), 891–896 (2004)

16. M.A. Kenawy, A.M. Abdel-Fattah, N. Okasha et al., Mechanical and structural properties of ductile cast iron. Egypt. J. Solids **24**(2), 151–159 (2001)